Full title: Brain oscillatory modes as a proxy of stroke recovery
Short title: Brain rhythms and stroke recovery

Authors:

Sylvain Harquel, PhD[1, 2,†]; Andéol Cadic-Melchior, MS[1, 2,†]; Takuya Morishita, PhD[1, 2]; Lisa Fleury, PhD[1,2]; Martino Ceroni, MS[1, 2]; Pauline Menoud, MS[1, 2]; Julia Brügger, PhD[1, 2]; Elena Beanato, MS[1, 2]; Nathalie Meyer, MS[3]; Giorgia G. Evangelista, PhD[1, 2]; Philip Egger, PhD[1, 2]; Dimitri Van de Ville, PhD[4, 5]; Olaf Blanke, PhD[8, 3]; Silvestro Micera, PhD[6, 7]; Bertrand Léger, PhD[9]; Jan Adolphsen, MD[10]; Caroline Jagella, MD[11]; Andreas Mühl, MD[9]; Christophe Constantin, MD[12]; Vincent Alvarez, MD[12]; Philippe Vuadens, MD[9]; Jean-Luc Turlan, MD[9]; Diego San Millán, MD[12]; Christophe Bonvin, MD[12];Philipp J. Koch, MD[1, 2,13]; Maximilian J. Wessel, MD[1, 2,14]; and Friedhelm C. Hummel, MD[1, 2,15*]

† These authors contributed equally to this work.

Affiliations:

[1] Defitech Chair of Clinical Neuroengineering, Neuro-X Institute (INX) and Brain Mind Institute (BMI), École Polytechnique Fédérale de Lausanne (EPFL), 1202 Geneva, Switzerland
[2] Defitech Chair of Clinical Neuroengineering, INX and BMI, EPFL Valais, Clinique Romande de Réadaptation, 1950 Sion, Switzerland
[3] Laboratory of Cognitive Neuroscience, INX and BMI, EPFL, 1202 Geneva, Switzerland
[4] Medical Image Processing Laboratory, Institute of Bioengineering, EPFL, 1202 Geneva, Switzerland
[5] Department of Radiology and Medical Informatics, University of Geneva (UNIGE), 1205 Geneva, Switzerland
[6] The Biorobotics Institute and Department of Excellence in Robotics & AI, Scuola Superiore Sant'Anna, Pisa, Italy
[7] Bertarelli Foundation Chair in Translational Neuroengineering, INX and Institute of Bioengineering, School of Engineering, Ecole Polytechnique Fédérale de Lausanne
[8] Department of Neurology, Geneva University Hospital (HUG), 1205 Geneva, Switzerland
[9] Clinique Romande de Réadaptation, 1950 Sion, Switzerland
[10] Mediclin Reha-Zentrum Plau am See, 19395 Plau am See, Germany
[11] Berner Klinik Montana, 3963 Crans-Montana, Switzerland
[12] Department of Neurology, Hôpital du Valais, 1950 Sion, Switzerland
[13] Department of Neurology, University of Lübeck, Lübeck, Germany
[14] Department of Neurology, Julius-Maximilians-University Würzburg, Würzburg, Germany
[15] Clinical Neuroscience, Geneva University Hospital, Geneva, Switzerland

*Corresponding author:
Prof. Dr. Friedhelm C. Hummel
Defitech Chair of Clinical Neuroengineering
Neuro-X Institute (INX) and Brain Mind Institute
École Polytechnique Fédérale de Lausanne (EPFL)
9 Chemin des Mines, 1202 Geneva, Switzerland
and
École Polytechnique Fédérale de Lausanne (EPFL Valais)
Clinique Romande de Réadaptation
Av. Grand-Champsec 90,
1951 Sion
Email: friedhelm.hummel@epfl.ch
Telephone: +41 21 69 35 440

Abstract:

Stroke is the leading cause of long-term disability, making the search for successful rehabilitation treatment one of the most important public health issues. A better understanding of the neural mechanisms underlying impairment and recovery and the development of associated markers is critical for tailoring treatments to each individual patient with the ultimate goal of maximizing therapeutic outcomes. Here, we used a novel and powerful method consisting of combined transcranial magnetic stimulation (TMS) and multichannel electroencephalography (EEG) to analyze TMS-induced brain oscillations in a large cohort of 60 stroke patients from the acute to the early-chronic phase after a stroke. A data-driven parallel factor analysis (PARAFAC) approach to tensor decomposition allowed to detect brain oscillatory modes specifically centered on the θ, α and β frequency bands. In the acute stage, patients presented a general slowdown of these oscillatory modes, highlighting stroke-induced perturbations within thalamocortical processing. Furthermore, low-frequency modes evolved across stroke stages, according to the extent of motor recovery, associated with changes in GABAergic intracortical inhibition. Overall, these longitudinal changes provide novel insights into the ongoing functional reorganization of brain networks after a stroke and the underlying mechanisms. Notably, we propose that the observed α-mode decrease corresponds to a beneficial disinhibition phase between the subacute and early-chronic stages that fosters structural and functional plasticity and facilitates recovery. Monitoring this phenomenon at the individual patient level will provide critical information for phenotyping patients, developing electrophysiological biomarkers and refining therapies based on personalized excitatory/inhibitory neuromodulation using noninvasive or invasive brain stimulation techniques.

Keywords:

Stroke, motor recovery, GABAergic disinhibition, alpha oscillations, TMS-EEG coupling

INTRODUCTION

Stroke is the leading cause of motor disability in the adult population. The exact mechanisms underlying motor impairment and recovery are the targets of a relentless search *(1–4)* but have yet to be elucidated in detail. Mechanistic knowledge is critical for designing and optimizing future patient-tailored rehabilitation protocols, in contrast to the current "one-size-fits-all" strategy adopted with limited success *(5–7)*. Neuroimaging tools have provided valuable insight in recent decades *(2, 6, 8, 9)*. Among these techniques, electroencephalography (EEG) allows us to explore the neural correlates of motor dysfunction with high temporal resolution *(10)*. Additionally, the identification of EEG-based biomarkers and predictors of motor impairment and recovery might be of particular interest, since these markers can easily be incorporated into clinical practice. A recent review by Keser *et al. (11)* included studies that explored the EEG correlates of motor function and recovery. Accumulated evidence suggested that stroke reduces high-frequency activity (> 8 Hz) and disrupts the balance of interhemispheric activity in the resting state or during a motor task. The majority of these findings are based on spectral features, highlighting the links of motor impairment and recovery with the alterations of baseline neural oscillatory patterns *(11)*. Another promising method of directly and causally probe the disruptions of brain oscillatory activity induced by the impaired motor system is to observe its immediate response after a brief and local perturbation through transcranial magnetic stimulation (TMS) *(12)*.

TMS-EEG coupling has recently gained interest in the field of clinical neuroscience *(13)* due to its vast application opportunities as a diagnostic tool in psychiatry, neurology, and (more specifically) in stroke *(11)*. Brain waves are the product of complex interactions between both local and remote neural oscillators *(14)*; thus, it is commonly accepted that the TMS pulse mainly acts as a phase reset, producing stronger oscillations thereafter *(15, 16)*. Compared with the resting state, this

subsequent increase in the signal-to-noise ratio is of great interest in regard to characterizing the brain dynamics, i.e., evoked neural oscillatory activity, of an area *(17, 18)* or the functional connectivity within – and between – brain networks *(11, 19)*. For example, TMS-EEG coupling enables identification of maladaptive interhemispheric functional connectivity between the two primary motor (M1) cortices in subacute and chronic stroke patients *(20–22)*; this maladaptive functional connectivity was not noticeable in the resting state *(11)*. Additionally, this coupling of methods adds to knowledge regarding stroke-induced modulation of neural oscillations. Recent cross-sectional research *(23, 24)* has indicated a reduction in response complexity in stroke patients, with an increase in low-frequency oscillations and a decrease in high-frequency oscillations. Such neurophysiological readouts might be markers of functional reorganization processes that enable motor recovery, especially among the thalamocortical networks to which this technique is sensitive *(18, 23)*.

While all the above work relies on evoked activity, i.e., synchronous neural activity phase-locked to the stimulation, no study to date has specifically explored TMS-induced oscillations, i.e., non-phase-locked oscillatory activity *(16)*. Focusing on evoked oscillations excludes nonstationary brain activity *(16, 25)*, thus eliminating all sources of variability regarding oscillation latency and phase from one stimulation to another *(15, 16)*; however, this approach overlooks valuable information, especially in the context of stroke. In a seminal study with healthy subjects, Premoli *et al. (26)* explored TMS-induced oscillations over M1 and found specific patterns of oscillations in the α and ß bands. Furthermore, the authors revealed a link between these patterns and the modulation of gamma-aminobutyric acid (GABAergic) inhibitory system activity. Modulation of inhibitory processes within the ipsilesional M1 is thought to play an important role in motor recovery, although thus far it has been examined only in animal models or small cohorts of patients

(27–31). Exploration of these oscillations is therefore important in the context of stroke, especially when applied to a large longitudinal cohort.

TMS-induced oscillations might provide important insight into understanding stroke recovery; however, such analyses are challenging. The related datasets have high dimensionality and are best represented by multidimensional (3–5D) arrays called tensors *(32)*. Tensors may include dimensions of space (electrodes or reconstructed sources), time, frequency, patients and even experimental sessions. Data-driven approaches capable of reducing such complex tensors into a simpler collection of parsimonious and unique components, or modes, have been developed (e.g., *30*) and tested in the EEG domain *(32)*, notably in the detection of epileptic seizures *(34, 35)*. Among these approaches, the parallel factor analysis (PARAFAC) algorithm *(33)* has recently been applied to TMS-EEG coupling data *(37, 38)*. The authors of these two studies were able to extract three to four brain oscillatory modes from the TMS-induced oscillations in M1 that were physiologically meaningful.

Interestingly, these modes did not overlap in frequency; instead, each was primarily driven by one main oscillatory pattern in the θ, α or β band. One of the observed modes was mainly driven by the θ band over the stimulated M1 and peaked approximately 200 ms after the TMS pulse *(37, 38)*. Such late and local activity might well be the signature of feedback from remote areas engaged after the indirect activation of cortico-cortical and cortico-subcortical networks *(12, 19)*. Studying the evolution of this oscillatory mode in the context of stroke might be important, since this low-frequency band has been associated with interregional communication supporting cognition in humans and animals *(39–41)*, which is heavily impacted in brain network diseases *(2, 11)*. Another mode focused on α activity, which is maximal over parieto-occipital *(38)* and stimulated motor areas *(37)*. By choosing a wider time window for analysis, Tangwiriyasakul *et al. (35)* showed that

this late activity was sustained up to 850 ms after the stimulation. As variations within α-band activity are linked with functional inhibitory processes *(42–47)* and such late TMS-induced α oscillations were mediated by the GABAergic system *(26)*, studying the α-band mode is of particular interest for determining the evolution of inhibitory processes in the time course of post-stroke motor recovery. The last extracted mode corresponded to the sensorimotor β-band activity generated by the stimulated motor cortex, consisting of an early burst (< 50 ms) of activity followed by a rebound 400 ms later *(38)*. This time course is the signature of the local activation of highly excitable pyramidal cells in layer V that are connected to the pyramidal tract leading to motor responses *(48)*, and the specific cytoarchitecture of M1 being prone to produce β-band activity *(17, 49)*. Interestingly, Belardinelli *et al. (34)* linked the β-band mode with glutamatergic activity, thus attracting additional interest regarding its relevance to stroke, given the importance of the evolution of the excitatory/inhibitory balance in motor recovery *(50)*.

In the present study, we sought to elucidate the mechanisms underlying motor impairment and recovery after stroke by applying this powerful method to stroke cases for the first time. We studied the changes in brain oscillatory modes unveiled from TMS-induced oscillations and determined their importance for residual motor functions and recovery. The present analyses are based on a large dataset from the TiMeS protocol *(51)*, a multimodal, multidomain, longitudinal evaluation of stroke patients from the acute to the subacute and early-chronic stage. We used the PARAFAC approach to extract brain oscillatory modes and to study their disruption with respect to motor impairment at the acute stage of stroke as well as changes during the course of motor recovery.

MATERIALS AND METHODS

Study design

This work is part of the TiMeS project, a detailed description of which is provided in Fleury et al., *2022*. TMS-induced oscillations and behavior were assessed at three different time points, one week (referred to here as "acute stage", A), three weeks ("subacute stage", SA) and three months poststroke ("early-chronic stage", EC, Fig. 1A). Seventy-six stroke patients participated in the study after being admitted to the Regional Hospital of Sion (HVS), Switzerland. Among them, 60 (age: 66.9 ± 13.3 years; 18 females) were included in this study, i.e., patients with TMS-EEG recordings at least in the first recording session (A stage). There were a variety of reasons that patients were unable to attend a recording session, including poor health, lack of motivation for participating in follow-up sessions, and the coronavirus disease 2019 (COVID-19) pandemic. Additionally, 19 healthy young adults (age: 26.9 ± 2.9 years, 9 females) and 15 healthy old adults (aged-matched with patients, age: 67 ± 5 years, 11 females) were recruited and underwent a single TMS-EEG recording session. The inclusion criteria were as follows: older than 18 years of age, no contraindications for MRI or TMS, and (for the patient group) motor deficits of the upper limb. The exclusion criteria included cognitive inability to provide informed consent, history of seizures, pregnancy, severe neuropsychiatric or medical diseases, regular use of narcotic drugs or medication that significantly interact with TMS, implanted medical electronic devices or ferromagnetic metal implants incompatible with MRI or TMS, and the request not to be informed in case of incidental findings. The study was conducted in accordance with the Declaration of Helsinki and was approved by Cantonal Ethics Committee Vaud, Switzerland (project number: 2018-01355). Written informed consent was obtained from all participants.

Behavioral data

At each time point, the bilateral motor capability (and impairment) of patients were assessed using (i) the Fugl-Meyer Assessment (FM) of the upper body (without reflexes), of the upper extremity (FM-UE), of the hand and of the wrist *(52)*, (ii) the maximum fist, key and pinch force, (iii) the box and blocks test, and (iv) the nine-hole peg test *(53)*. The maximum grip forces were assessed in three trials using a JAMAR® hydraulic hand dynamometer *(54)*. The ratio between the affected and the nonaffected hand was used as the primary outcome for the grip forces and scores on the box and blocks and nine-hole peg tests. Change ratios between time points were computed for each motor measurement *x* as follows (e.g. A vs. SA): $(x_{SA} - x_A)/x_A$.

The electrophysiological features were globally inspected over the whole patient cohort and specifically over the subgroup of recovering patients. Patients were classified as "recovering" if they exhibited an improvement in FM-UE scores from the A stage to the SA stage or from the A/SA stages to the EC stage.

TMS-EEG acquisition

The details of the acquisition parameters can be found in our previous paper *(55)* that analyzed TMS-evoked potentials. In brief, 64-channel TMS-compatible EEG (BrainAmp DC amplifiers, Brain Products GmbH, Germany) was recorded concurrently with the neuronavigated (Localite GmbH, Germany) stimulation of the ipsilesional motor cortex over the first dorsal interosseous (FDI) motor hotspot using an MC-B70 coil connected to a MagPro X100 stimulator (MagVenture A/S, Denmark). A total of 180 suprathreshold single-pulse stimulations were delivered. If no motor activity was evoked from the lesioned hemisphere, the stimulation parameters were tuned to the contralesional hemisphere. DC and low-pass (1 kHz) filtered EEG was sampled at 5 kHz, and the

electrode impedance level was kept below 5 kΩ. During the stimulation, the patient was instructed to remain still while staring at a fixation cross and listening to white noise through noise-canceling earphones to limit eye movements and the influence of the TMS click sound on the EEG signal.

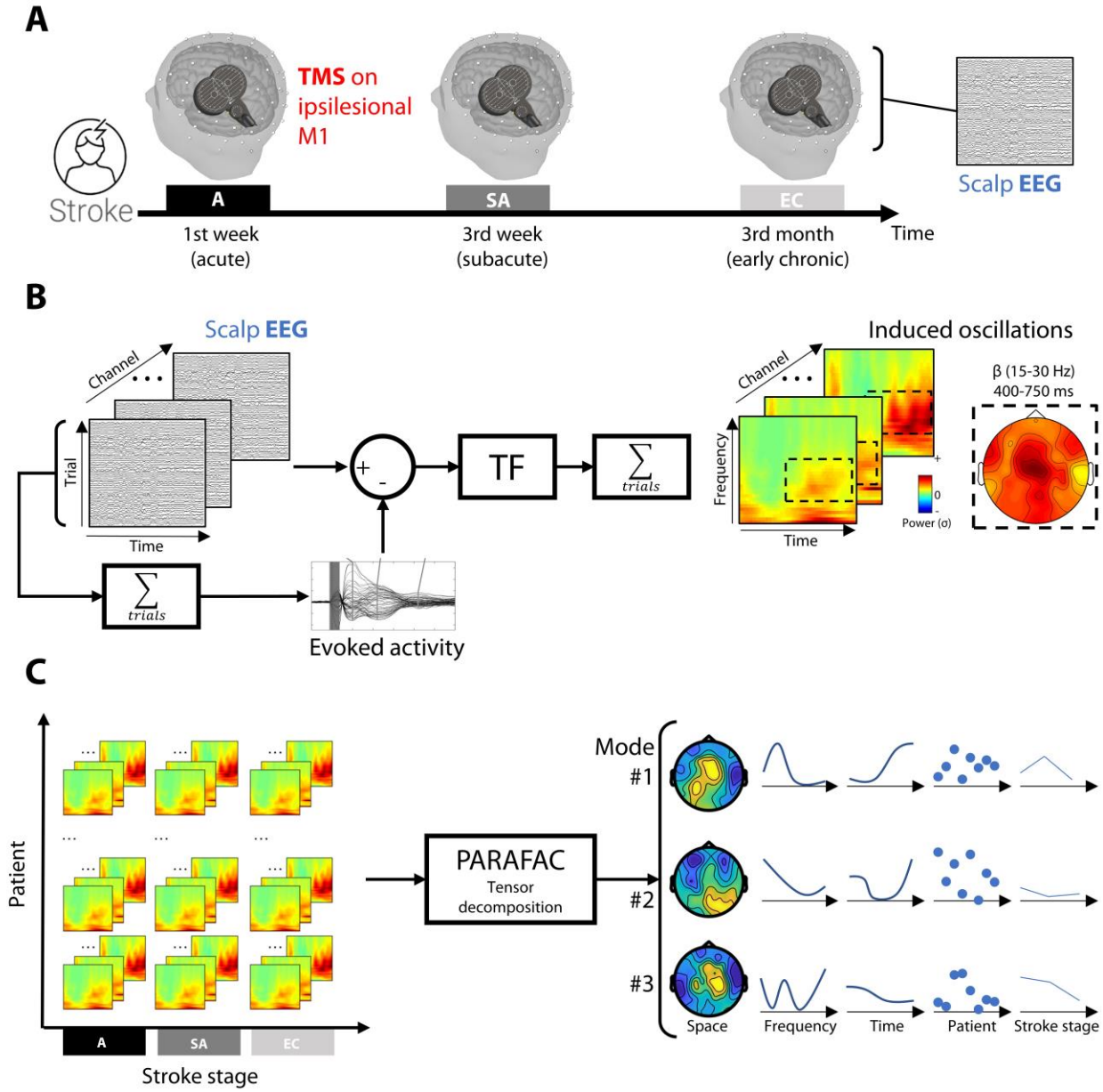

Fig. 1: Protocol design and main data processing pipeline. (**A**). Protocol design including 3 TMS-EEG coupling sessions during the 1st week, 3rd week and 3rd month after stroke (referred to as the acute, subacute and early-chronic stages, respectively). (**B**). Signal processing pipeline for computing induced oscillation maps. For each patient and channel, the evoked activity (average

of the clean signal across trials) was removed from the clean signal prior to the time-frequency (TF) transform. Each TF map was z transformed with baseline values (-200 to -50 ms prior to TMS pulse) before averaging across trials. Examples of induced oscillation maps (+40 to +750 ms; 7 to 40 Hz) and the topography of late central β oscillations are depicted on the right for one representative patient. (**C**). Tensor decomposition using the PARAFAC approach. Induced oscillation maps were compiled into a tensor, with the patient and stroke stages as the 4th and 5th dimensions, respectively, and decomposed using the PARAFAC algorithm. This decomposition led to several components, or modes, whose weights are represented in the space (topography), frequency, time, patient and stroke-stage dimensions, from left to right.

TMS-EEG analysis

The analysis methodology used in this study was adapted from Tangwiriyasakul *et al. (35)*, in which the PARAFAC tensor decomposition approach was applied for the first time to TMS-EEG data.

Preprocessing

TMS-EEG data were analyzed with MATLAB (The MathWorks, USA) and preprocessed using the EEGLAB *(56)* and TESA *(57)* toolboxes. The clean datasets analyzed in this study were identical to those in our previously published paper *(55)*. In short, raw TMS-EEG data were preprocessed using a double independent component analysis (ICA) *(58)* to remove components linked to pulse, muscle, decay and ocular artifacts from the data. The preprocessed dataset resulted in an average of 149 ± 24 cleaned trials epoched from -500 to +1,000 ms around the TMS pulse and filtered between 1 and 80 Hz.

Induced oscillations

Induced oscillations were computed in MATLAB using the Fieldtrip toolbox *(59)* (Fig. 1B). First, the TMS-evoked potentials (TEPs) were computed by averaging all trials and were then individually subtracted from the signal in each trial to filter out evoked activity *(60)*. Then, the time-frequency (TF) map of each corrected trial was computed using a multitapers approach. The signal from the -500 to +1,000 ms time window (10-ms step) was convoluted with Hanning tapers ranging from 7 to 40 Hz (1-Hz step), with a width of 3.5 cycles per window. For each electrode and trial, the resulting power time series was normalized using the z-score against baseline (-200 to -50 ms), before being averaged across trials to obtain the final TF maps. . Prior to tensor definition, all the TF maps were flipped as needed so that the ipsilesional hemisphere was defined as the left for all patients.

PARAFAC tensor decomposition

Regarding the patient database, four different tensors were constructed to answer the study's main questions as follows: the first tensor focused on the A stage (4D: electrode × frequency × time × patient), while the second to the fourth tensors gathered the induced oscillations across stroke stages (A vs. SA stage, A vs. EC stage, and from A to EC stage; 5D: electrode × frequency × time × patient × stroke stage) (Fig. 1C). For each tensor, the TF maps were cropped between +40 and +750 ms to prevent missing values from boundary effects, resulting in a size of 62 × 34 × 70 for the first three dimensions. A total of 60, 43, 33 and 27 patients were included at the A stage, the A and SA stages, the A and EC stages, and all stages, respectively; thus, the final sizes of the four tensors were as follows: first tensor (A stage only), 62 × 34 × 70 × 60 (8,853,600 datapoints); second tensor (A vs. SA stage), 62 × 34 × 70 × 43 × 2 (12,690,160 datapoints); third tensor (A vs. EC stage), 62 × 34 × 70 × 33 × 2 (9,738,960 datapoints); and fourth tensor (A to EC; all stages),

62 × 34 × 70 × 27 × 3 (11,952,360 datapoints). The link between brain oscillatory modes and motor recovery was further inspected by splitting the last 5D tensor into two parts: the first subtensor comprised only stable patients, while the second comprised recovering patients. Regarding healthy adults, the final tensors of the young and aged-matched groups were 62 × 34 × 70 × 19 or 15 respectively (2,803,640 or 2,213,400 datapoints).

Statistical analysis

Differences between stroke stages when decomposing the 5D tensors were assessed using the same permutation-based approach proposed in *(38)*. In short, 1,000 surrogate tensors were obtained by permuting data from the 4th and 5th dimensions (patient and stroke-stage dimensions) while keeping the data structure unchanged over the 3 first dimensions. A PARAFAC decomposition was then performed on each surrogate tensor using the old loadings of the original data decomposition in the first three dimensions, i.e., forcing the extracted modes to be identical to the original data in the space, frequency and time dimensions. The corresponding mean differences between stroke stages (differences between data in the 5th dimension) were gathered across all decompositions to form the surrogate data distributions. Differences between time points (A vs. SA, A vs. EC and SA vs. EC) within each brain mode (θ, α and β modes) in the original tensors were considered significant if greater or lower than 2.5% of these surrogate distributions ($p < 0.05$, two-sided). This alpha level was Bonferroni corrected in order to account for multiple testing (1 or 3 differences × 3 modes = 3 or 9, for tensors including 2 or 3 stroke stages respectively), which led to a corrected threshold of 0.83% or 0.25% respectively (referred as $p_{Bonf} < 0.05$ in the text).

The link between patient weights (data in the 4th dimension) within the extracted modes and motor scores was explored using the Bayesian equivalent of nonparametric Kendall correlation testing

using JASP software (JASP Team - 2022). The weights of each extracted mode were compared with the initial motor scores in the A stage and to the change ratio between stroke stages (see *Behavioral data*). The default values proposed within the JASP framework were used to keep the priors regarding effect sizes relatively large. Correlation values were reported using the 95% confidence interval of Kendall's τ, while the statistical evidence of the tests was reported using Bayes factors (BF_{10}) and the cutoff values defined by Jeffreys (1998) for interpretation.

Data availability

The data related to this article and all custom scripts and JASP files are available upon reasonable request from the corresponding author.

RESULTS

All 60 patients, whose characteristics are detailed in Table 1, underwent longitudinal TMS-EEG evaluations without any adverse events. The lesion heatmap of the patient cohort at inclusion is depicted in Fig. 2. Overall, patients recovered from their stroke-induced motor impairment from the acute to the early-chronic stages, exhibiting average reductions in motor impairment of 7.7 points on the FM–UE. Specifically, stroke patients exhibited improved motor functions, such as performance on the box and blocks and nine-hole peg tests; reduced spasticity, with an average decrease of 1.7 points on the Modified Ashworth Scale (MAS); and improved autonomy, with an average increase of 10.8 points on the Barthel Scale (Table 1). These motor improvements were also accompanied by cognitive improvements, leading to an average increase of 3.2 points on the Montreal Cognitive Assessment (MoCA).

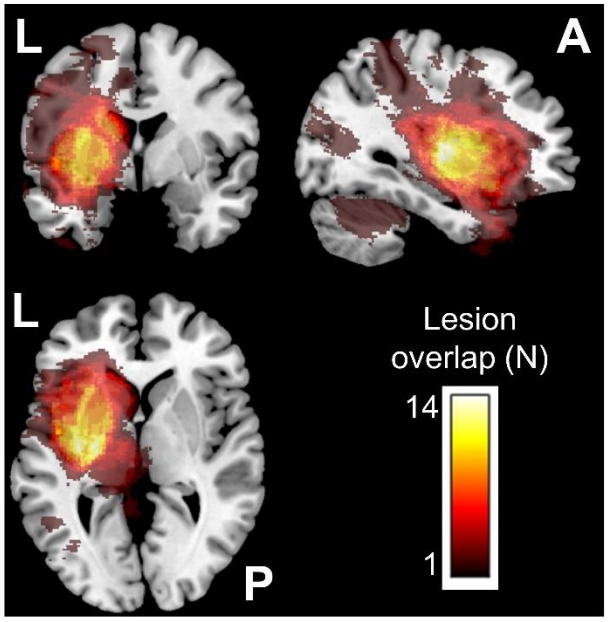

Fig. 2: Lesion heatmap of patients at the acute (or subacute, if data unavailable) stage, N = 54. Right-hemispheric lesions were flipped to the left side. Note that 6 out of 60 patients did not undergo magnetic resonance imaging (MRI) at the acute or subacute stages.

Table 1: Patient characteristics.

Sex	Age (years)	Handedness	Hemisphere affected	Resting Motor Threshold (% MSO)	Days poststroke			FM–UE score (/60)			NIHSS score		
				Acute	Acute	Subacute	Early-chronic	Acute	Subacute	Early-chronic	Acute	Subacute	Early-chronic
18 F/ 42 M	66.9 ± 13.3	54 right-handed	30 Left/ 30 right	43 ± 10	6.6 ± 2.3	27 ± 5	98.6 ± 8.8	47.3 ± 18.5	50.9 ± 16.5	55 ± 12.1	5.7 ± 5.4	2.0 ± 3.0	0.6 ± 1.3

MAS score (/48)			MoCA score (/30)			Barthel Scale score (/100)			Box and blocks test score (aff./nonaff.)			Nine-hole peg test score (aff./nonaff.)		
Acute	Subacute	Early-chronic	Acute	Subacute	Early-chronic	Acute	Subacute	Early-chronic	Acute	Subacute	Early-chronic	Acute	Subacute	Early-chronic
3 ± 5.6	2.5 ± 4.9	1.3 ± 2.4	22.7 ± 4.9	24.1 ± 4.9	25.9 ± 3.5	88.2 ± 19.5	93.8 ± 13	99 ± 3.1	0.74 ± 0.34	0.79 ± 0.31	0.89 ± 0.23	2.6 ± 2.4	2.1 ± 2.2	1.6 ± 1.6

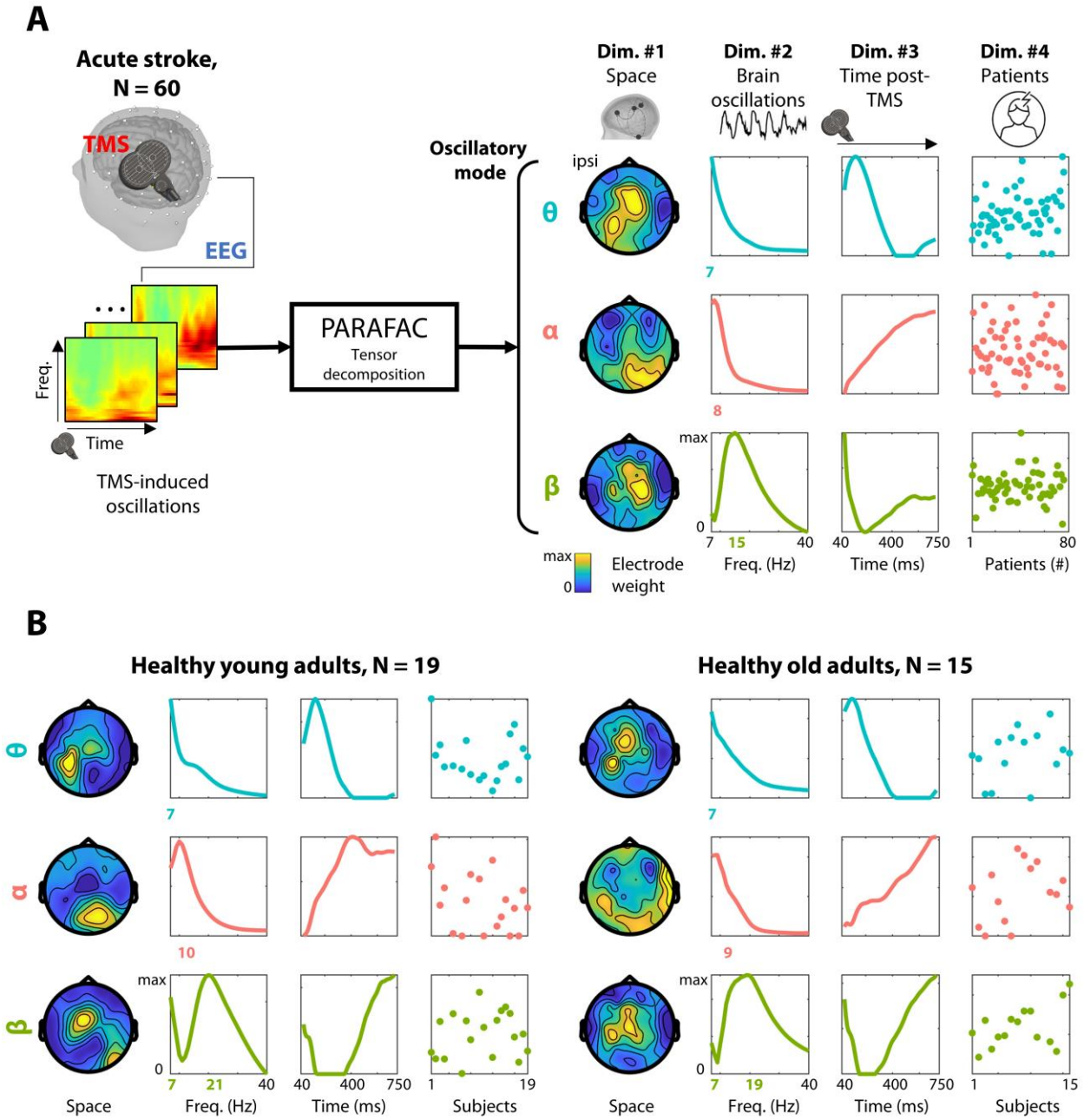

Fig. 3: Brain oscillatory modes extracted from stroke patients and healthy adults. (**A**) PARAFAC decomposition of the 4D tensor of the TMS-induced oscillations in acute stroke patients. Modes are sorted by row according to their main frequency peak, from θ (7 Hz, blue) and α (8 and 10 Hz, red) to high β (15 and 21 Hz, green) frequency bands (top to bottom). Each column depicts the relative weights (from 0 to maximum) of each mode in the space, frequency, time and patient dimensions (from left to right). The mode frequency peak is highlighted in color

on the y-axis. Data were flipped for patients whose lesion was located on the right hemisphere so that the ipsilesional side was the left side. (**B**) Results of the same tensor decomposition in healthy young (left) and old (right) adults, with similar sorting of modes.

Perturbation of brain oscillatory modes in acute stroke patients

Fig. 3 shows the induced oscillatory modes obtained after the 4D tensor decomposition in A patients (N = 60) and in healthy young (N = 19) and old adults (N = 15). The three identified modes were similar among the three groups; however, A patients presented an overall slowdown of brain oscillatory activity, indicated by a decrease in the peak frequency of the different modes. The first mode was centered on θ oscillations (7-Hz peak) distributed over the stimulation site, i.e., the ipsilesional hemisphere, which corresponds to central and central left electrodes (right-lesioned data were flipped for analysis purposes). The mode peaked at approximately 80 ms, followed by a decrease until 400 ms. The second mode converged on the parieto-occipital α waves that emerged over time starting 150-200 ms after stimulation, with healthy young adults presenting a steeper increase than older adults and A patients. The main frequency of this mode was lower in A patients (8 Hz) than in healthy young (10 Hz) and older adults (9 Hz). The third mode mainly focused on central sensorimotor β and μ waves. The peak frequency differed among the three groups: A patients presented one peak at 15 Hz, while healthy young adults showed two peaks at 7 and 21 Hz, and older adults showed one peak at 19 Hz. Finally, the overall time course of these β oscillations was the same, with one early peak at 40 ms followed by a decrease and a rebound after 400 ms. However, the early peak activity was more pronounced in A patients, whereas the rebound was stronger in both healthy adult groups.

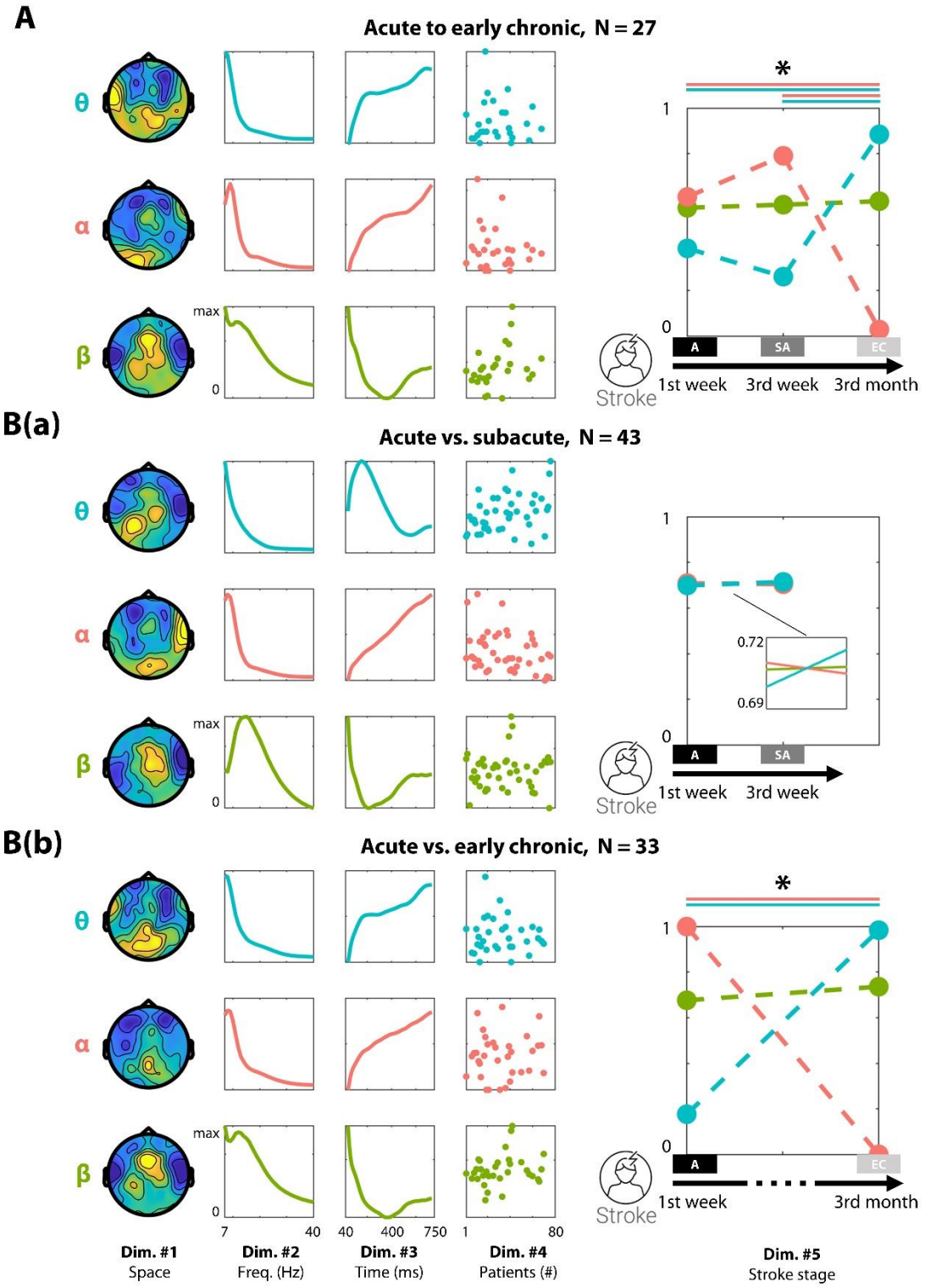
A
Acute to early chronic, N = 27
θ
α
β
max
0
*
1
0
A
SA
EC
Stroke
1st week
3rd week
3rd month
B(a)
Acute vs. subacute, N = 43
0.72
0.69
B(b)
Acute vs. early chronic, N = 33
7
40
40
400
750
1
80
Dim. #1
Space
Dim. #2
Freq. (Hz)
Dim. #3
Time (ms)
Dim. #4
Patients (#)
Dim. #5
Stroke stage

Fig. 4: **Evolution of brain oscillatory modes from acute to early-chronic stages**. (**A**) PARAFAC decomposition of the 5D tensor in all patients leading to 3 main modes. The modes are sorted by peak frequency, from θ (blue) and α (red) to β (green) bands. Each column depicts the relative weights (from 0 to maximum) of each mode in the space, frequency, time, patient and stroke-stage dimensions (from left to right). The asterisk and colored lines indicate significant effects of the pairwise comparisons of the stroke stages within the θ (blue lines) and α (red lines) modes for the acute (A) vs. early-chronic (EC) stages and the subacute (SA) vs. early-chronic (EC) stages (permutation test, $p_{Bonf} < 0.05$, see *Statistical analysis*). (**B**). The results of the same decomposition, run separately on the A and SA stages **(a)** and on the A and EC stages **(b)**. Note that mode weights overlap on the y-axis (0-1 scale) for A vs. SA (**B(a)**). Taken together, the results indicate that there were changes in the θ and α-band modes over time, especially large changes in the θ and α-band modes from A to EC, but no changes in the β-band mode in general.

Evolution of brain oscillatory modes over the time course of recovery

The results of the decomposition of the 5D tensors including all stroke stages (A, SA, and EC) are presented in Fig. 4. The 5D tensors included all patients who were systematically recorded at each required stage. The differences between stroke stages were assessed using a permutation-based approach (see *Statistical analysis*). Overall, the three first modes extracted by PARAFAC were of the same nature as those obtained using the 4D tensor at the A stage (Fig. 4A, N = 27). However, both the spectra and time courses were less specific after the addition of the most remote session (EC, three months after stroke onset) within the 5th dimension and the modes started to overlap within these dimensions. In particular, the β and α spectra were less specific, with flatter spectral peaks covering wider frequency bands. The time course of β oscillations was less contrasted

between peaks and troughs, while α and θ bands overlapped and followed the same pattern as the one previously described for the α-band mode (Fig. 3).

Interestingly, the mode weights were significantly modulated across stroke stages (permutation tests, $p_{Bonf} < 0.05$, N = 27, see Fig. S1 for detailed results). This change was specific to α- and θ-band modes that significantly differed from the A and the SA stage to the EC stage with opposite directions and different strengths across stages. While the relative weight of the α-band mode increased at the SA stage before decreasing at the EC stage, the θ-band mode modulated in the opposite direction with a decrease at the SA stage followed by an increase at the EC stage. Overall, the changes were much stronger at the EC stage, which was confirmed in larger groups of patients by pairwise comparisons between A and the two later stroke stages. No change was found for any of the modes when comparing the A to the SA stage (N = 43, Fig. 4B(a)), whereas a strong increase and decrease in the θ and α-band modes, respectively, was found in the EC stage (permutation tests, $p_{Bonf} < 0.05$, N = 33, Fig. 4B(b)). Finally, no significant modulation of the β-band mode through stroke stages was found in any of the tensor decompositions.

Modulation of brain oscillatory modes as a proxy of motor recovery

We further explored the modulation across stroke stages by distinguishing patients who actually recovered along the evaluated stroke stages (recovering group) from patients who maintained stable motor functions since their inclusion at the A stage (stable group, for group definitions please see *Materials and Methods*). Overall, the three modes were of the same nature in the first 3 dimensions, but the two groups drastically diverged regarding the modulation across stroke stages (5th dimension, Fig. 5A). These data indicate that the previously observed modulations were mainly driven by the recovering group, in which the same significant effects were observed

between subacute and early-chronic stages (permutation tests, N = 17, $p_{Bonf} < 0.05$; see Fig. 5A, right, compare with Fig. 4A), whereas no change was noticeable within the stable group between stroke stages (permutation test, N = 10; Fig. 5A, left).

All tensor decompositions showed variability in the weights of modes among patients, i.e., within the 4th dimension. We next aimed to explain the variability among patients in terms of impairment, function and recovery, e.g., upper limb motor function, gross and fine dexterity, impairment and changes over the recovery process, by linking this variability with the different modes and their changes (Fig. 5B). No statistical evidence was found for either a link or an absence of links between θ- and β-band modes on motor scores or their modulation through stroke stages (Bayesian Kendall correlation, N = 17, all $1/3 < BF_{10} < 3$) in any of the tested patient cohorts (full, only stable or only recovering patients). However, moderate to strong statistical evidence was found for a link between the α-band mode and motor scores in the A stage and its evolution across the SA and EC stages in the recovering group (Fig. 5B). First, patients who exhibited a stronger weight associated with this α-band mode were more impaired in the A stage (Fig. 5B(a)), with lower FM hand scores in the A stage (N = 17, $\tau = [-0.09\ -0.7]$, $BF_{10} = 7.3$). Stronger association with the α-mode was also found in better recovering patients between the A and SA stages (Fig. 5B(b)), as revealed by a stronger change ratio between the A and SA stages in the FM hand ($\tau = [0.22\ 0.8]$, $BF_{10} = 91$), wrist ($\tau = [0.05\ 0.65]$, $BF_{10} = 3.9$), and total scores ($\tau = [0.07\ 0.67]$, $BF_{10} = 5.8$) as well as the maximum fist force ($\tau = [0.07\ 0.67]$, $BF_{10} = 5.9$). The stronger the patients were associated to this α-band mode, the better they improved at the SA stage. Finally, a similar association was found in the longer term, with stronger change ratios between the A and EC stages in scores on the FM hand ($\tau = [0.2\ 0.8]$, $BF_{10} = 56$), BnB ($\tau = [0.08\ 0.7]$, $BF_{10} = 6.0$) and nine-hole peg tests ($\tau = [-0.08$

-0.7], BF_{10} = 6.0) (Fig. 5B(c)), indicating that greater changes in the α-band mode were associated with larger improvements in motor functions and thus larger reductions in impairment.

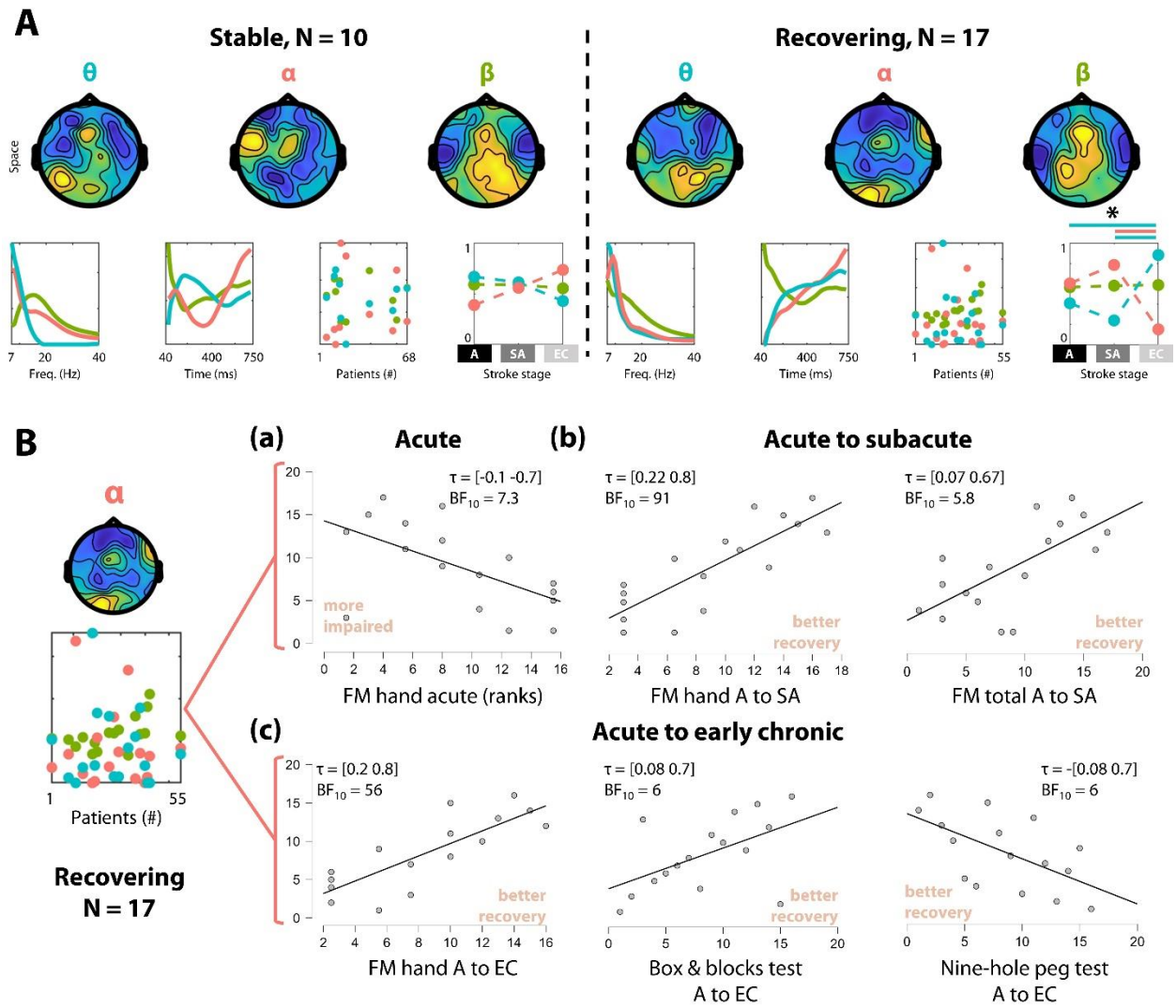

Fig. 5. Links among brain oscillatory modes, motor impairment and motor recovery. (**A**). PARAFAC decomposition of the 5D tensor in stable (left) and recovering (right) patients (see Fig. 3). (**B**) Association between the α-band mode and motor scores (FM and performance on the box & block and nine-hole peg tests) in the recovering group. The Kendall rank correlation coefficient (τ) and Bayesian factors (BF_{10}) are indicated for each comparison, and all data are plotted according to their rank (see *Statistical analysis*). (**a**). Moderate evidence of an anticorrelation

between α-band mode and motor impairment in the acute stage indicates that a more positive α-band mode in the acute stage led to more impairment. (**b**). Moderate to strong evidence of a correlation between α-band mode and changes in motor impairment to the subacute stage indicates that the greater the change in the α-band mode, the larger the reduction in impairment. (**c**). Moderate to strong evidence of correlations between α-band mode and changes in motor functions and impairment to the early-chronic stage indicate that the greater the change in the α-band mode, the better the improvement in motor functions, and the larger the reduction in impairment.

DISCUSSION

In the present study, we report longitudinal (A to EC stage) changes in induced oscillatory activity modes in a large cohort of stroke patients by means of TMS-EEG coupling as well as the association of these changes in induced oscillations with functional motor recovery. The results highlight dynamic changes in correlates of inhibitory activity, shifting from enhanced inhibitory activity in the acute stage to recovery-supporting disinhibition from the subacute to the early chronic stage (Fig. 6).

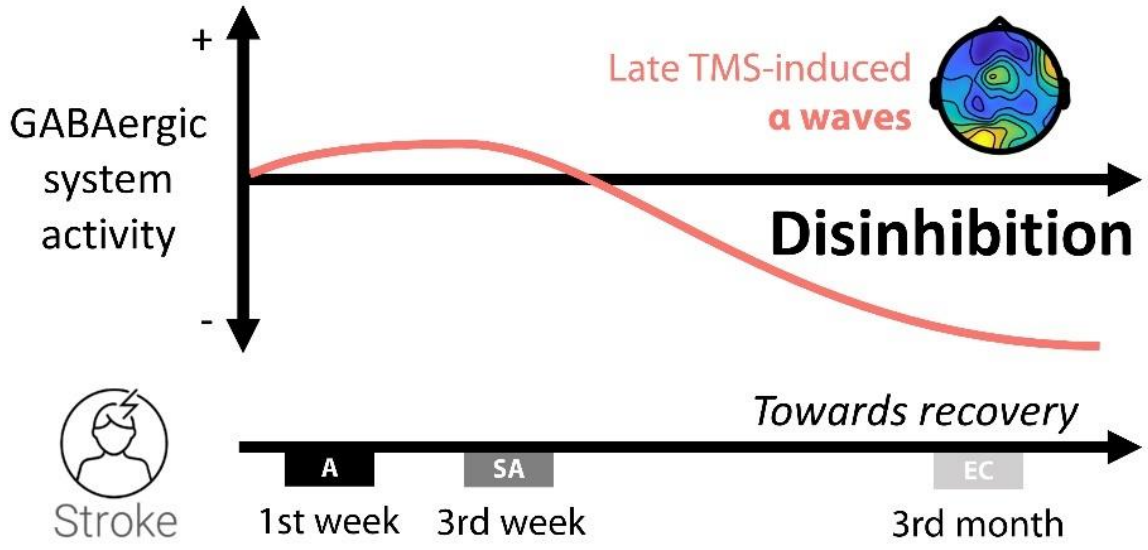

Fig. 6. Time course of GABAergic inhibition and its relationship with recovery. The decrease in the TMS-induced late α waves (corresponding to GABAergic activity) from an initially high level represents a global and recovery-facilitating functional disinhibition after a detrimental hyperinhibitory period in the A stage. This disinhibition fosters structural and functional plasticity that support motor recovery toward the early-chronic stage.

Slowdown of brain oscillatory modes in the acute phase after a stroke

The decomposition of TMS-induced oscillations in stroke patients revealed several discrepancies in brain dynamics occurring in the acute stage. The most noticeable was the global slowdown of oscillatory patterns in stroke patients compared with healthy adults (Fig. 3). The majority of knowledge regarding the disruption of neural oscillatory activity induced by ischemic stroke comes from resting-state EEG studies *(11)*; accumulated evidence points to an increase in low (δ and θ) and a decrease in higher (α and β) frequency-band power *(62, 63)*. Notably, such slow EEG abnormalities were an accurate index for discriminating between acute patients and age-matched controls *(64)*. We extended these results by showing that the structural damage caused by stroke may have also changed the resonance frequency of brain oscillators; these alterations surpassed pure variations in spectral power within one frequency band or the ratio between several bands and could not be solely explained by normal aging (Fig. 3C). By taking advantage of the higher spatial resolution of magnetoencephalography (MEG), Tecchio and colleagues *(52)* found a similar slowdown within higher frequency bands between the unaffected and the affected hemisphere. The exact origin of induced oscillations is currently debated, but TMS is known to generate and amplify thalamocortical loop oscillations *(16, 18)*. This slowdown of high-frequency oscillations has also been observed using TMS-EEG coupling in several psychiatric pathologies and has been linked with a disruption of thalamocortical circuits *(66–68)*. A severe impairment of this cortical-subcortical functional connectivity in our cohort of patients is supported as the lesions were largely present in subcortical areas (Fig. 2).

Evolution of TMS-induced oscillations as a proxy of functional reorganization and its underlying mechanisms

To assess the evolution of the observed induced oscillatory patterns through the different stages of recovery, we added a 5th dimension to the tensors to encompass the longitudinal aspect of the present data. Decomposition of these tensors allowed us to observe interesting functional reorganization phenomena occurring between the acute and early chronic stages that were beneficial to motor recovery. The θ- and α-band modes were associated with significant changes over time, with their final weights in the early chronic stage compared to those in the acute and subacute stages increasing for the θ-band mode and decreasing for the α-band mode, when decomposition was performed on the three stages (Fig. 4A), or on only two of the three over larger groups of patients (Fig. 4B). Notably, the changes in θ- and α-band modes observed among stroke stages were mainly driven by the recovering patient group (Fig. 5A), in which the strength of the link was positively correlated with global and task-related motor recovery scores at the subacute and early chronic stages (Fig. 5B).

As θ oscillations are an important basis for interregional communication, the positive modulation of these oscillations during recovery might be the signature of the re-establishment of large-scale functional connectivity within the motor network to foster functional recovery. Growing evidence suggests that stroke, rather than simply inducing dysfunction localized to the lesioned area, has a direct impact on functional connectivity *(2)*, i.e., neural communication within connected brain areas. The disturbance of functional connectivity has been associated with proportional neurological deficits in stroke patients (see, e.g., *(61-63)*), and normalization of functional connectivity over time is linked with recovery (e.g., *(72, 73)*. Even though the increase in the θ oscillatory mode observed in the early chronic stage was not directly linked with motor scores,

this increase was observable when recovering patients were included in the data tensor, indicating normalization of interregional interactions. On the other hand, the longitudinal decrease observed in the α mode, together with the absence of any significant change within the β-band mode, may underline the importance of the evolution of the excitatory/inhibitory balance across stroke stages, with dominantly GABAergic activity changing compared to glutamatergic activity. This finding points to the existence of a beneficial disinhibition phase, especially in the recovering patient group, which will be discussed in the next section.

Previous studies have shown the importance of low-frequency oscillations, such as the δ and θ bands, in the lesioned hemisphere; these oscillations are linked with better motor recovery (for review, see *(11)*). Interestingly, this phenomenon was discovered by studying brain oscillations either in the resting state *(74)* or during an active state when patients were performing a visuomotor task *(75)*. However, findings in the resting state might not be functionally relevant, and the findings during tasks inevitably include the confounders of the individual level of task performance/impairment and the respective effort needed that both significantly impact oscillatory activity. In contrast, TMS-EEG coupling allows us to address both shortcomings by (a) a controlled input to the motor system that (b) is functionally meaningful. The use of TMS thus allows us to directly observe controlled brain oscillations that can be analyzed and classified either as *evoked* or *induced* by the stimulation, depending on whether one wishes to observe the result of coherent firing (evoked) or nonlinear interactions (induced) of neurons following the stimulus *(16, 25)*. By fully considering the variability in the phase and latency of the generated neural oscillations *(15)*, TMS-induced oscillations allow to increase the sensitivity of detecting stroke-related changes in brain dynamics. Last, induced oscillations are known to reflect higher-order processing *(76, 77)*, which is of particular importance when studying poststroke recovery. Thus,

the analysis of TMS-induced oscillations in the present study explained the observed variability in motor recovery of fine motor tasks, such as the nine-hole peg and box and blocks tests, which rely on higher-order motor processes, such as grasping and manipulation, that engage complex motor networks distributed among motor, premotor and parietal cortices, among others *(78)*.

Disinhibition supports motor recovery

The α-band modulations found here can be considered a proxy of the dynamic evolution of the intracortical inhibitory system, which has been suggested to sustain motor recovery *(28, 71)* (Fig. 6). As stated above, previous evidence has suggested that late TMS-induced oscillations occurring in the α band are linked with GABAergic-mediated inhibition *(26)*. Immediately after stroke, during the hyperacute phase, hyperinhibition of the perilesional cortical areas prevents additional tissue damage due to ischemia-induced excitotoxicity *(80–82)*. However, the persistence of hyperinhibition over time was correlated with worse motor outcomes *(27, 28)*, and pharmacological reduction in GABAergic inhibition led to better recovery in animal models *(27, 83, 84)*. Further evidence has confirmed this last point by linking better motor recovery with a period of plasticity driven by molecular changes, such as cellular excitability *(85)*, or by sustained disinhibition during the first weeks poststroke. This disinhibition has been suggested to promote functional reorganization within the lesioned hemisphere *(79, 80, 86)*. Consistent with this suggestion, the initially high α-band mode weights in the acute to subacute stages observed in the present study may be the signature of the enduring and detrimental nature of GABA-mediated hyperinhibition, as revealed by its association with acute residual motor functions. Furthermore, the decrease in the α-band mode in the recovering patient group is most likely a correlate of the

disinhibition between the subacute and early chronic stages (three weeks to three months poststroke), which supports the recovery process.

The time frame of this phenomenon is somewhat coherent with the previous findings of Liuzzi *et al. (28)*, in which disinhibition occurred from the first days to up to three weeks after stroke onset. Although this previous work studied only a very small and homogenous mildly impaired patient group, the slight differences in the precise timing of this effect might also stem from the brain areas represented by the specific measures. While the short-interval intracortical inhibition protocol used by Liuzzi *et al. (28)* allows measurement of the intracortical GABAergic activity locally within the motor cortex, the late induced α oscillations in the present work are linked with inhibitory activity at a more global scale, i.e., engaged in higher-order processes within larger-scale brain networks (see above). The disinhibition phenomenon might first occur locally within the lesioned motor cortex in the subacute stage before spreading to larger areas to promote functional plasticity more broadly and thus support more complex motor (and cognitive) functions in later stages. Since patients presenting these particular changes in inhibitory activity over time exhibited greater motor improvement (Fig. 5B), our results support the idea that the exact timing of the inhibitory evolution after stroke is important for the extent of motor recovery *(28)*. Finally, the absence of change in α activity in stable patients (Fig. 5A) might be the signature of the normalization of inhibitory activity. In this patient group, a beneficial disinhibition phase might have already occurred earlier and transiently, explaining their stable and high motor function upon their inclusion in the study. Overall, these results strongly support the view that changes in inhibitory activity play differential functional roles in the excitatory/inhibitory balance, ranging from hyperinhibition in the acute stage, which protects tissues from further damage *(50)*, to strong disinhibition in the early chronic phase, which promotes functional recovery *(28)*.

Limitations

Despite the exciting opportunities that the present analytical method provides, there are a few limitations worth mentioning, namely, the number of modes extracted, the lack of a sham stimulation condition, and the variation in the patient cohort. The number of modes extracted was an arbitrary decision. However, fixing this number to 3 appeared to be the best choice for the following reasons. First, this number was a good trade-off between achieving a plateau of at least 50% of explained variance while preventing worse diagnosis regarding the proportion of variation effectively explained by a multidimensional linear phenomenon, as the corcondia value *(87)* was already weak (15%) or null (see SOM and Table S1). Second, the 3 computed components were physiologically meaningful in all five analyses, with the extra components constituting only the repetition or overlap of the three first components, as also found earlier by *(38)*. Secondly, all recent guidelines about TMS-EEG coupling acquisition and data processing were followed in this work, with the exception of the presence of a realistic sham stimulation condition in order to assess the influence of peripheral evoked potentials, due to the multisensory features of TMS, on the recorded EEG signal *(88, 89)*. However, since the present work is based on TMS-induced oscillations, which are computed after removing such evoked components from the signal, and on a longitudinal analysis approach, the lack of sham stimulation condition does not affect the final interpretation of our results. Finally, another limitation is the distribution of our patient cohort with respect to the severity of motor impairment in the acute stage and the extent of recovery. Most of the patients were rather mildly impaired. Additional analyses of more heterogeneous groups in the future will help to refine the present conclusions regarding the link between changes in brain oscillatory modes and motor recovery.

Conclusion

In summary, examining a large cohort of stroke patients over time using TMS-EEG coupling provided a better understanding of the neural mechanisms linked to motor recovery. The present results support the existence of a disinhibition phase between the subacute and early chronic stages that is beneficial for motor recovery. The acquired knowledge might pave the way for developing novel biomarkers to determine and predict stroke recovery and to personalize innovative therapies based on modulation of brain oscillatory activity through noninvasive or invasive brain stimulation.

Acknowledgments

We thank the Center for Biomedical Imaging, a Swiss research center of excellence, and the MRI and neuromodulation facilities of the Human Neuroscience Platform of the Fondation Campus Biotech Geneva and the Neuroimaging Center of the Sion Hospital for their expertise and access to their facilities.

Funding

This work was supported by grants from the 'Personalized Health and Related Technologies (PHRT-#2017-205)' of the ETH Domain (CH), the Defitech Foundation (Strike-the-Stroke project, Morges, CH), the SNSF (NIBS-iCog, 320030L_197899 / 1) and the Wyss Center for Bio- and Neuroengineering (WP030; Geneva, CH).

Competing interests

The authors report that they have no competing interests.

References and notes:

1. C. Grefkes, G. R. Fink, Recovery from stroke: current concepts and future perspectives. *Neurol Res Pract* **2**, 17 (2020).

2. A. G. Guggisberg, P. J. Koch, F. C. Hummel, C. Buetefisch, Brain networks and their relevance for stroke rehabilitation. *Clin Neurophysiol* **130**, 1098–1124 (2019).

3. E. Raffin, F. C. Hummel, Restoring Motor Functions After Stroke: Multiple Approaches and Opportunities. *Neuroscientist* **24**, 400–416 (2018).

4. D. Smajlović, Strokes in young adults: epidemiology and prevention. *Vasc Health Risk Manag* **11**, 157–164 (2015).

5. M. Coscia, M. J. Wessel, U. Chaudary, J. D. R. Millán, S. Micera, A. Guggisberg, P. Vuadens, J. Donoghue, N. Birbaumer, F. C. Hummel, Neurotechnology-aided interventions for upper limb motor rehabilitation in severe chronic stroke. *Brain* **142**, 2182–2197 (2019).

6. P. J. Koch, F. C. Hummel, Toward precision medicine: tailoring interventional strategies based on noninvasive brain stimulation for motor recovery after stroke. *Current Opinion in Neurology* **30**, 388–397 (2017).

7. S. Micera, M. Caleo, C. Chisari, F. C. Hummel, A. Pedrocchi, Advanced Neurotechnologies for the Restoration of Motor Function. *Neuron* **105**, 604–620 (2020).

8. L. A. Boyd, K. S. Hayward, N. S. Ward, C. M. Stinear, C. Rosso, R. J. Fisher, A. R. Carter, A. P. Leff, D. A. Copland, L. M. Carey, L. G. Cohen, D. M. Basso, J. M. Maguire, S. C. Cramer, Biomarkers of stroke recovery: Consensus-based core recommendations from the Stroke Recovery and Rehabilitation Roundtable. *Int J Stroke* **12**, 480–493 (2017).

9. C. Grefkes, G. R. Fink, Connectivity-based approaches in stroke and recovery of function. *Lancet Neurol* **13**, 206–216 (2014).

10. P. L. Nunez, R. Srinivasan, *Electric Fields of the Brain: The Neurophysics of EEG* (Oxford University Press, 2006).

11. Z. Keser, S. C. Buchl, N. A. Seven, M. Markota, H. M. Clark, D. T. Jones, G. Lanzino, R. D. Brown, G. A. Worrell, B. N. Lundstrom, Electroencephalogram (EEG) With or Without Transcranial Magnetic Stimulation (TMS) as Biomarkers for Post-stroke Recovery: A Narrative Review. *Front. Neurol.* **13**, 827866 (2022).

12. H. R. Siebner, K. Funke, A. S. Aberra, A. Antal, S. Bestmann, R. Chen, J. Classen, M. Davare, V. Di Lazzaro, P. T. Fox, M. Hallett, A. N. Karabanov, J. Kesselheim, M. Malling Beck, G. Koch, D. Liebetanz, S. Meunier, C. Miniussi, W. Paulus, A. V. Peterchev, T. Popa, M. C. Ridding, A. Thielscher, U. Ziemann, J. C. Rothwell, Y. Ugawa, Transcranial magnetic stimulation of the brain: What is stimulated? – a consensus and critical position paper. *Clinical Neurophysiology* (2022), doi:10.1016/j.clinph.2022.04.022.

13. S. Tremblay, N. C. Rogasch, I. Premoli, D. M. Blumberger, S. Casarotto, R. Chen, V. Di Lazzaro, F. Farzan, F. Ferrarelli, P. B. Fitzgerald, J. Hui, R. J. Ilmoniemi, V. K. Kimiskidis, D. Kugiumtzis, P. Lioumis, A. Pascual-Leone, M. C. Pellicciari, T. Rajji, G. Thut, R. Zomorrodi, U. Ziemann, Z. J. Daskalakis, Clinical utility and prospective of TMS–EEG. *Clinical Neurophysiology* **130**, 802–844 (2019).

14. X.-J. Wang, Neurophysiological and Computational Principles of Cortical Rhythms in Cognition. *Physiological Reviews* **90**, 1195–1268 (2010).

15. V. Moliadze, Y. Zhao, U. Eysel, K. Funke, Effect of transcranial magnetic stimulation on single-unit activity in the cat primary visual cortex. *The Journal of Physiology* **553**, 665–679 (2003).

16. M. C. Pellicciari, D. Veniero, C. Miniussi, Characterizing the Cortical Oscillatory Response to TMS Pulse. *Front Cell Neurosci* **11**, 38 (2017).

17. S. Harquel, T. Bacle, L. Beynel, C. Marendaz, A. Chauvin, O. David, Mapping dynamical properties of cortical microcircuits using robotized TMS and EEG: Towards functional cytoarchitectonics. *Neuroimage* **135**, 115–124 (2016).

18. M. Rosanova, A. Casali, V. Bellina, F. Resta, M. Mariotti, M. Massimini, Natural Frequencies of Human Corticothalamic Circuits. *Journal of Neuroscience* **29**, 7679–7685 (2009).

19. M. Bortoletto, D. Veniero, G. Thut, C. Miniussi, The contribution of TMS–EEG coregistration in the exploration of the human cortical connectome. *Neuroscience & Biobehavioral Reviews* **49**, 114–124 (2015).

20. M. R. Borich, L. A. Wheaton, S. M. Brodie, B. Lakhani, L. A. Boyd, Evaluating interhemispheric cortical responses to transcranial magnetic stimulation in chronic stroke: A TMS-EEG investigation. *Neurosci Lett* **618**, 25–30 (2016).

21. E. P. Casula, M. C. Pellicciari, S. Bonnì, B. Spanò, V. Ponzo, I. Salsano, G. Giulietti, A. M. Cinnera, M. Maiella, I. Borghi, L. Rocchi, M. Bozzali, F. Sallustio, C. Caltagirone, G. Koch, Evidence for interhemispheric imbalance in stroke patients as revealed by combining transcranial magnetic stimulation and electroencephalography. *Human Brain Mapping* **42**, 1343–1358 (2021).

22. J. A. Palmer, L. A. Wheaton, W. A. Gray, M. A. Saltão da Silva, S. L. Wolf, M. R. Borich, Role of Interhemispheric Cortical Interactions in Poststroke Motor Function. *Neurorehabil Neural Repair* **33**, 762–774 (2019).

23. M. C. Pellicciari, S. Bonnì, V. Ponzo, A. M. Cinnera, M. Mancini, E. P. Casula, F. Sallustio, S. Paolucci, C. Caltagirone, G. Koch, Dynamic reorganization of TMS-evoked activity in subcortical stroke patients. *NeuroImage* **175**, 365–378 (2018).

24. C. Tscherpel, S. Dern, L. Hensel, U. Ziemann, G. R. Fink, C. Grefkes, Brain responsivity provides an individual readout for motor recovery after stroke. *Brain* **143**, 1873–1888 (2020).

25. T. Mutanen, TMS-evoked changes in brain-state dynamics quantified by using EEG data. *Frontiers in Human Neuroscience* **7** (2013), doi:10.3389/fnhum.2013.00155.

26. I. Premoli, T. O. Bergmann, M. Fecchio, M. Rosanova, A. Biondi, P. Belardinelli, U. Ziemann, The impact of GABAergic drugs on TMS-induced brain oscillations in human motor cortex. *NeuroImage* **163**, 1–12 (2017).

27. A. N. Clarkson, B. S. Huang, S. E. MacIsaac, I. Mody, S. T. Carmichael, Reducing excessive GABA-mediated tonic inhibition promotes functional recovery after stroke. *Nature* **468**, 305–309 (2010).

28. G. Liuzzi, V. Horniss, P. Lechner, J. Hoppe, K. Heise, M. Zimerman, C. Gerloff, F. C. Hummel, Development of movement-related intracortical inhibition in acute to chronic subcortical stroke. *Neurology* **82**, 198–205 (2014).

29. F. C. Hummel, B. Steven, J. Hoppe, K. Heise, G. Thomalla, L. G. Cohen, C. Gerloff, Deficient intracortical inhibition (SICI) during movement preparation after chronic stroke. *Neurology* **72**, 1766–1772 (2009).

30. J. U. Blicher, J. Near, E. Næss-Schmidt, C. J. Stagg, H. Johansen-Berg, J. F. Nielsen, L. Østergaard, Y.-C. L. Ho, GABA levels are decreased after stroke and GABA changes during rehabilitation correlate with motor improvement. *Neurorehabil Neural Repair* **29**, 278–286 (2015).

31. J. Cirillo, R. A. Mooney, S. J. Ackerley, P. A. Barber, V. M. Borges, A. N. Clarkson, C. Mangold, A. Ren, M.-C. Smith, C. M. Stinear, W. D. Byblow, Neurochemical balance and inhibition at the subacute stage after stroke. *J Neurophysiol* **123**, 1775–1790 (2020).

32. F. Cong, Q.-H. Lin, L.-D. Kuang, X.-F. Gong, P. Astikainen, T. Ristaniemi, Tensor decomposition of EEG signals: a brief review. *J Neurosci Methods* **248**, 59–69 (2015).

33. T. G. Kolda, B. W. Bader, Tensor Decompositions and Applications. *SIAM Rev.* **51**, 455–500 (2009).

34. Y. R. Aldana, B. Hunyadi, E. J. M. Reyes, V. R. Rodriguez, S. Van Huffel, Nonconvulsive Epileptic Seizure Detection in Scalp EEG Using Multiway Data Analysis. *IEEE J Biomed Health Inform* **23**, 660–671 (2019).

35. W. Deburchgraeve, P. J. Cherian, M. De Vos, R. M. Swarte, J. H. Blok, G. H. Visser, P. Govaert, S. Van Huffel, Neonatal seizure localization using PARAFAC decomposition. *Clin Neurophysiol* **120**, 1787–1796 (2009).

36. R. A. Harshman, FOUNDATIONS OF THE PARAFAC PROCEDURE: MODELS AND CONDITIONS FOR AN “EXPLANATORY” MULTIMODAL FACTOR ANALYSIS. , 84.

37. P. Belardinelli, F. König, C. Liang, I. Premoli, D. Desideri, F. Müller-Dahlhaus, P. C. Gordon, C. Zipser, C. Zrenner, U. Ziemann, TMS-EEG signatures of glutamatergic neurotransmission in human cortex. *Sci Rep* **11**, 8159 (2021).

38. C. Tangwiriyasakul, I. Premoli, L. Spyrou, R. F. Chin, J. Escudero, M. P. Richardson, Tensor decomposition of TMS-induced EEG oscillations reveals data-driven profiles of antiepileptic drug effects. *Sci Rep* **9**, 17057 (2019).

39. R. T. Canolty, E. Edwards, S. S. Dalal, M. Soltani, S. S. Nagarajan, H. E. Kirsch, M. S. Berger, N. M. Barbaro, R. T. Knight, High gamma power is phase-locked to theta oscillations in human neocortex. *Science* **313**, 1626–1628 (2006).

40. E. A. Solomon, J. E. Kragel, M. R. Sperling, A. Sharan, G. Worrell, M. Kucewicz, C. S. Inman, B. Lega, K. A. Davis, J. M. Stein, B. C. Jobst, K. A. Zaghloul, S. A. Sheth, D. S. Rizzuto, M. J. Kahana, Widespread theta synchrony and high-frequency desynchronization underlies enhanced cognition. *Nat Commun* **8**, 1704 (2017).

41. A. J. Watrous, N. Tandon, C. R. Conner, T. Pieters, A. D. Ekstrom, Frequency-specific network connectivity increases underlie accurate spatiotemporal memory retrieval. *Nat Neurosci* **16**, 349–356 (2013).

42. F. Hummel, F. Andres, E. Altenmüller, J. Dichgans, C. Gerloff, Inhibitory control of acquired motor programmes in the human brain. *Brain* **125**, 404–420 (2002).

43. O. Jensen, A. Mazaheri, Shaping Functional Architecture by Oscillatory Alpha Activity: Gating by Inhibition. *Frontiers in Human Neuroscience* **4** (2010) (available at https://www.frontiersin.org/article/10.3389/fnhum.2010.00186).

44. W. Klimesch, P. Sauseng, S. Hanslmayr, EEG alpha oscillations: the inhibition-timing hypothesis. *Brain Res Rev* **53**, 63–88 (2007).

45. G. Pfurtscheller, A. Stancák, C. Neuper, Event-related synchronization (ERS) in the alpha band--an electrophysiological correlate of cortical idling: a review. *Int J Psychophysiol* **24**, 39–46 (1996).

46. P. Sauseng, W. Klimesch, K. F. Heise, W. R. Gruber, E. Holz, A. A. Karim, M. Glennon, C. Gerloff, N. Birbaumer, F. C. Hummel, Brain oscillatory substrates of visual short-term memory capacity. *Curr Biol* **19**, 1846–1852 (2009).

47. G. Thut, A. Nietzel, S. A. Brandt, A. Pascual-Leone, Alpha-band electroencephalographic activity over occipital cortex indexes visuospatial attention bias and predicts visual target detection. *J Neurosci* **26**, 9494–9502 (2006).

48. A. S. Aberra, B. Wang, W. M. Grill, A. V. Peterchev, Simulation of transcranial magnetic stimulation in head model with morphologically-realistic cortical neurons. *Brain Stimulation* **13**, 175–189 (2020).

49. J. J. Bouyer, M. F. Montaron, J. M. Vahnée, M. P. Albert, A. Rougeul, Anatomical localization of cortical beta rhythms in cat. *Neuroscience* **22**, 863–869 (1987).

50. S. T. Carmichael, Brain excitability in stroke: the yin and yang of stroke progression. *Arch Neurol* **69**, 161–167 (2012).

51. L. Fleury, P. J. Koch, M. J. Wessel, C. Bonvin, D. S. Millan, C. Constantin, P. Vuadens, J. Adolphsen, A. G. Cadic-Melchior, J. Brügger, E. Beanato, M. Ceroni, P. Menoud, D. de L. Rodriguez, V. Zufferey, N. Meyer, P. Egger, S. Harquel, T. Popa, E. Raffin, G. Girard, J. P. Thiran, C. Vaney, V. Alvarez, J.-L. Turlan, A. Mühl, B. Leger, T. Morishita, S. Micera, O. Blanke, D. V. de Ville, F. C. Hummel, Towards individualized Medicine in Stroke – the TiMeS project: protocol of longitudinal, multi-modal, multi-domain study in stroke, 2022.05.18.22274612 (2022).

52. A. R. Fugl-Meyer, L. Jääskö, I. Leyman, S. Olsson, S. Steglind, A method for evaluation of physical performance. *Scand J Rehabil Med* **7**, 13–31 (1975).

53. V. Mathiowetz, G. Volland, N. Kashman, K. Weber, Adult norms for the Box and Block Test of manual dexterity. *The American journal of occupational therapy* **39**, 386–391 (1985).

54. V. Mathiowetz, K. Weber, G. Volland, N. Kashman, Reliability and validity of grip and pinch strength evaluations. *The Journal of hand surgery* **9**, 222–226 (1984).

55. A. Cadic-Melchior, S. Harquel, T. Morishita, L. Fleury, A. Witon, M. Ceroni, J. Bruegger, N. Meyer, G. Evangelista, P. Egger, E. Beanato, P. Menoud, D. V. D. Ville, S. Micera, O. Blanke, B. Leger, J. Adolphsen, C. Jagella, C. Constantin, V. Alvarez, P. Vuadens, J.-A. Ghika, J.-L. Turlan, A. Muhl, D. S. Millan, C. Bonvin, P. J. Koch, M. Wessel, F. C. Hummel, Stroke recovery related changes in brain reactivity based on modulation of intracortical inhibition, 2022.09.20.22280144 (2022).

56. A. Delorme, S. Makeig, EEGLAB: an open source toolbox for analysis of single-trial EEG dynamics including independent component analysis. *Journal of neuroscience methods* **134**, 9–21 (2004).

57. N. C. Rogasch, C. Sullivan, R. H. Thomson, N. S. Rose, N. W. Bailey, P. B. Fitzgerald, F. Farzan, J. C. Hernandez-Pavon, Analysing concurrent transcranial magnetic stimulation and electroencephalographic data: A review and introduction to the open-source TESA software. *Neuroimage* **147**, 934–951 (2017).

58. N. C. Rogasch, R. H. Thomson, F. Farzan, B. M. Fitzgibbon, N. W. Bailey, J. C. Hernandez-Pavon, Z. J. Daskalakis, P. B. Fitzgerald, Removing artefacts from TMS-EEG recordings using independent component analysis: Importance for assessing prefrontal and motor cortex network properties. *NeuroImage* **101**, 425–439 (2014).

59. R. Oostenveld, P. Fries, E. Maris, J.-M. Schoffelen, FieldTrip: Open Source Software for Advanced Analysis of MEG, EEG, and Invasive Electrophysiological Data. *Computational Intelligence and Neuroscience* **2011**, 1–9 (2011).

60. M. X. Cohen, T. H. Donner, Midfrontal conflict-related theta-band power reflects neural oscillations that predict behavior. *Journal of Neurophysiology* **110**, 2752–2763 (2013).

61. H. Jeffreys, *The Theory of Probability* (OUP Oxford, 1998).

62. S. Finnigan, M. J. A. M. van Putten, EEG in ischaemic stroke: quantitative EEG can uniquely inform (sub-)acute prognoses and clinical management. *Clin Neurophysiol* **124**, 10–19 (2013).

63. K. G. Jordan, Emergency EEG and continuous EEG monitoring in acute ischemic stroke. *J Clin Neurophysiol* **21**, 341–352 (2004).

64. S. Finnigan, A. Wong, S. Read, Defining abnormal slow EEG activity in acute ischaemic stroke: Delta/alpha ratio as an optimal QEEG index. *Clin Neurophysiol* **127**, 1452–1459 (2016).

65. F. Tecchio, F. Zappasodi, P. Pasqualetti, M. Tombini, C. Salustri, A. Oliviero, V. Pizzella, F. Vernieri, P. M. Rossini, Rhythmic brain activity at rest from rolandic areas in acute mono-hemispheric stroke: A magnetoencephalographic study. *NeuroImage* **28**, 72–83 (2005).

66. P. Canali, S. Sarasso, M. Rosanova, S. Casarotto, G. Sferrazza-Papa, O. Gosseries, M. Fecchio, M. Massimini, M. Mariotti, R. Cavallaro, E. Smeraldi, C. Colombo, F. Benedetti, Shared reduction of oscillatory natural frequencies in bipolar disorder, major depressive disorder and schizophrenia. *Journal of Affective Disorders* **184**, 111–115 (2015).

67. F. Ferrarelli, S. Sarasso, Y. Guller, B. A. Riedner, M. J. Peterson, M. Bellesi, M. Massimini, B. R. Postle, G. Tononi, Reduced natural oscillatory frequency of frontal thalamocortical circuits in schizophrenia. *Arch. Gen. Psychiatry* **69**, 766–774 (2012).

68. F. Ferrarelli, M. Massimini, M. Peterson, B. Riedner, M. Lazar, M. Murphy, R. Huber, M. Rosanova, A. Alexander, N. Kalin, Reduced evoked gamma oscillations in the frontal cortex in schizophrenia patients: a TMS/EEG study. *American Journal of Psychiatry* **165**, 996–1005 (2008).

69. M. A. Urbin, X. Hong, C. E. Lang, A. R. Carter, Resting-state functional connectivity and its association with multiple domains of upper-extremity function in chronic stroke. *Neurorehabil Neural Repair* **28**, 761–769 (2014).

70. M. Allegra, C. Favaretto, N. Metcalf, M. Corbetta, A. Brovelli, Stroke-related alterations in inter-areal communication. *Neuroimage Clin* **32**, 102812 (2021).

71. A. R. Carter, S. V. Astafiev, C. E. Lang, L. T. Connor, J. Rengachary, M. J. Strube, D. L. W. Pope, G. L. Shulman, M. Corbetta, Resting interhemispheric functional magnetic resonance imaging connectivity predicts performance after stroke. *Ann Neurol* **67**, 365–375 (2010).

72. A.-M. Golestani, S. Tymchuk, A. Demchuk, B. G. Goodyear, VISION-2 Study Group, Longitudinal evaluation of resting-state FMRI after acute stroke with hemiparesis. *Neurorehabil Neural Repair* **27**, 153–163 (2013).

73. J. Wu, E. B. Quinlan, L. Dodakian, A. McKenzie, N. Kathuria, R. J. Zhou, R. Augsburger, J. See, V. H. Le, R. Srinivasan, S. C. Cramer, Connectivity measures are robust biomarkers of cortical function and plasticity after stroke. *Brain* **138**, 2359–2369 (2015).

74. M. Bönstrup, L. Krawinkel, R. Schulz, B. Cheng, J. Feldheim, G. Thomalla, L. G. Cohen, C. Gerloff, Low-Frequency Brain Oscillations Track Motor Recovery in Human Stroke. *Ann Neurol* **86**, 853–865 (2019).

75. J. M. Cassidy, A. Wodeyar, J. Wu, K. Kaur, A. K. Masuda, R. Srinivasan, S. C. Cramer, Low Frequency Oscillations Are A Biomarker Of Injury And Recovery After Stroke. *Stroke* **51**, 1442–1450 (2020).

76. D. Henao, M. Navarrete, M. Valderrama, M. Le Van Quyen, Entrainment and synchronization of brain oscillations to auditory stimulations. *Neuroscience Research* **156**, 271–278 (2020).

77. C. Tallon-Baudry, O. Bertrand, C. Delpuech, J. Pernier, Stimulus Specificity of Phase-Locked and Non-Phase-Locked 40 Hz Visual Responses in Human. *J. Neurosci.* **16**, 4240–4249 (1996).

78. A. Errante, S. Ziccarelli, G. Mingolla, L. Fogassi, Grasping and Manipulation: Neural Bases and Anatomical Circuitry in Humans. *Neuroscience* **458**, 203–212 (2021).

79. R. A. Mooney, S. J. Ackerley, D. K. Rajeswaran, J. Cirillo, P. A. Barber, C. M. Stinear, W. D. Byblow, The Influence of Primary Motor Cortex Inhibition on Upper Limb Impairment and Function in Chronic Stroke: A Multimodal Study. *Neurorehabil Neural Repair* **33**, 130–140 (2019).

80. A. N. Clarkson, B. S. Huang, S. E. Macisaac, I. Mody, S. T. Carmichael, Reducing excessive GABA-mediated tonic inhibition promotes functional recovery after stroke. *Nature* **468**, 305–309 (2010).

81. G. Michalettos, K. Ruscher, Crosstalk Between GABAergic Neurotransmission and Inflammatory Cascades in the Post-ischemic Brain: Relevance for Stroke Recovery. *Front Cell Neurosci* **16**, 807911 (2022).

82. G. Rabiller, J.-W. He, Y. Nishijima, A. Wong, J. Liu, Perturbation of Brain Oscillations after Ischemic Stroke: A Potential Biomarker for Post-Stroke Function and Therapy. *Int J Mol Sci* **16**, 25605–25640 (2015).

83. R. Lamtahri, M. Hazime, E. K. Gowing, R. Y. Nagaraja, J. Maucotel, M. Alasoadura, P. P. Quilichini, K. Lehongre, B. Lefranc, K. Gach-Janczak, A.-B. Marcher, S. Mandrup, D. Vaudry, A. N. Clarkson, J. Leprince, J. Chuquet, The Gliopeptide ODN, a Ligand for the Benzodiazepine Site of GABAA Receptors, Boosts Functional Recovery after Stroke. *J Neurosci* **41**, 7148–7159 (2021).

84. F. Lebrun, N. Violle, A. Letourneur, C. Muller, N. Fischer, A. Levilly, C. Orset, A. Sors, D. Vivien, Post-acute delivery of α5-GABAA antagonist, S 44819, improves functional recovery in juvenile rats following stroke. *Experimental Neurology* **347**, 113881 (2022).

85. M. T. Joy, S. T. Carmichael, Encouraging an excitable brain state: mechanisms of brain repair in stroke. *Nat Rev Neurosci* **22**, 38–53 (2021).

86. G. Liuzzi, V. Hörniß, P. Lechner, J. Hoppe, K. Heise, M. Zimerman, C. Gerloff, F. C. Hummel, Development of movement-related intracortical inhibition in acute to chronic subcortical stroke. *Neurology* **82**, 198–205 (2014).

87. R. Bro, H. A. L. Kiers, A new efficient method for determining the number of components in PARAFAC models. *Journal of Chemometrics* **17**, 274–286 (2003).

88. V. Conde, L. Tomasevic, I. Akopian, K. Stanek, G. B. Saturnino, A. Thielscher, T. O. Bergmann, H. R. Siebner, The non-transcranial TMS-evoked potential is an inherent source of ambiguity in TMS-EEG studies. *NeuroImage* **185**, 300–312 (2019).

89. P. Belardinelli, M. Biabani, D. M. Blumberger, M. Bortoletto, S. Casarotto, O. David, D. Desideri, A. Etkin, F. Ferrarelli, P. B. Fitzgerald, A. Fornito, P. C. Gordon, O. Gosseries, S. Harquel, P. Julkunen, C. J. Keller, V. K. Kimiskidis, P. Lioumis, C. Miniussi, M. Rosanova, S. Rossi, S. Sarasso, W. Wu, C. Zrenner, Z. J. Daskalakis, N. C. Rogasch, M. Massimini, U. Ziemann, R. J. Ilmoniemi, Reproducibility in TMS–EEG studies: a call for data sharing, standard procedures and effective experimental control. *Brain Stimulation* (2019), doi:10.1016/j.brs.2019.01.010.

Figure legends

Fig. 1: Protocol design and main data processing pipeline. (**A**). Protocol design including 3 TMS-EEG coupling sessions during the 1st week, 3rd week and 3rd month after stroke (referred to as the acute, subacute and early-chronic stages, respectively). (**B**). Signal processing pipeline for computing induced oscillation maps. For each patient and channel, the evoked activity (average of the clean signal across trials) was removed from the clean signal prior to the time-frequency (TF) transform. Each TF map was z transformed with baseline values (-200 to -50 ms prior to TMS pulse) before averaging across trials. Examples of induced oscillation maps (+40 to +750 ms; 7 to 40 Hz) and the topography of late central β oscillations are depicted on the right for one representative patient. (**C**). Tensor decomposition using the PARAFAC approach. Induced oscillation maps were compiled into a tensor, with the patient and stroke stages as the 4th and 5th dimensions, respectively, and decomposed using the PARAFAC algorithm. This decomposition led to several components, or modes, whose weights are represented in the space (topography), frequency, time, patient and stroke-stage dimensions, from left to right.

Fig. 2: Lesion heatmap of patients at the acute (or subacute, if data unavailable) stage, N = 54. Right-hemispheric lesions were flipped to the left side. Note that 6 out of 60 patients did not undergo magnetic resonance imaging (MRI) at the acute or subacute stages.

Fig. 3: Brain oscillatory modes extracted from stroke patients and healthy adults. (**A**) PARAFAC decomposition of the 4D tensor of the TMS-induced oscillations in acute stroke patients. Modes are sorted by row according to their main frequency peak, from θ (7 Hz, blue) and α (8 and 10 Hz, red) to high β (15 and 21 Hz, green) frequency bands (top to bottom). Each column depicts the relative weights (from 0 to maximum) of each mode in the space, frequency, time and patient dimensions (from left to right). The mode frequency peak is highlighted in color on the y-axis. Data were flipped for patients whose lesion was located on the right hemisphere so

that the ipsilesional side was the left side. (**B**) Results of the same tensor decomposition in healthy young (left) and old (right) adults, with similar sorting of modes.

Fig. 4: **Evolution of brain oscillatory modes from acute to early-chronic stages**. (**A**) PARAFAC decomposition of the 5D tensor in all patients leading to 3 main modes. The modes are sorted by peak frequency, from θ (blue) and α (red) to β (green) bands. Each column depicts the relative weights (from 0 to maximum) of each mode in the space, frequency, time, patient and stroke-stage dimensions (from left to right). The asterisk and colored lines indicate significant effects of the pairwise comparisons of the stroke stages within the θ (blue lines) and α (red lines) modes for the acute (A) vs. early-chronic (EC) stages and the subacute (SA) vs. early-chronic (EC) stages (permutation test, $p_{Bonf} < 0.05$, see *Statistical analysis*). (**B**). The results of the same decomposition, run separately on the A and SA stages **(a)** and on the A and EC stages **(b)**. Note that mode weights overlap on the y-axis (0-1 scale) for A vs. SA (**B(a)**). Taken together, the results indicate that there were changes in the θ and α-band modes over time, especially large changes in the θ and α-band modes from A to EC, but no changes in the β-band mode in general.

Fig. 5. Links among brain oscillatory modes, motor impairment and motor recovery. (**A**). PARAFAC decomposition of the 5D tensor in stable (left) and recovering (right) patients (see Fig. 3). (**B**) Association between the α-band mode and motor scores (FM and performance on the box & block and nine-hole peg tests) in the recovering group. The Kendall rank correlation coefficient (τ) and Bayesian factors (BF_{10}) are indicated for each comparison, and all data are plotted according to their rank (see *Statistical analysis*). (**a**). Moderate evidence of an anticorrelation between α-band mode and motor impairment in the acute stage indicates that a more positive α-band mode in the acute stage led to more impairment. (**b**). Moderate to strong evidence of a correlation between α-band mode and changes in motor impairment to the subacute stage indicates that the greater the change in the α-band mode, the larger the reduction in impairment.

(**c**). Moderate to strong evidence of correlations between α-band mode and changes in motor functions and impairment to the early-chronic stage indicate that the greater the change in the α-band mode, the better the improvement in motor functions, and the larger the reduction in impairment.

Fig. 6. Time course of GABAergic inhibition and its relationship with recovery. The decrease in the TMS-induced late α waves (corresponding to GABAergic activity) from an initially high level represents a global and recovery-facilitating functional disinhibition after a detrimental hyperinhibitory period in the A stage. This disinhibition fosters structural and functional plasticity that support motor recovery toward the early-chronic stage.